

Net 321.24-Gb/s IMDD Transmission Based on a >100-GHz Bandwidth Directly-Modulated Laser

Nikolaos-Panteleimon Diamantopoulos^{1,*}, Hiroshi Yamazaki^{1,2}, Suguru Yamaoka¹, Munehiko Nagatani^{1,2}, Hidetaka Nishi¹, Hiromasa Tanobe³, Ryo Nakao¹, Takuro Fujii¹, Koji Takeda¹, Takaaki Kakitsuka^{1,4}, Hitoshi Wakita¹, Minoru Ida¹, Hideyuki Nosaka^{1,2}, Fumio Koyama⁵, Yutaka Miyamoto², Shinji Matsuo¹

¹NTT Device Technology Labs, NTT corporation, Atsugi, Kanagawa, Japan

²NTT Network Innovation Labs, NTT corporation, Yokosuka, Kanagawa, Japan

³NTT Device Innovation Center, NTT corporation, Atsugi, Kanagawa, Japan

⁴now with Graduate School of Information, Production and Systems, Waseda University, Kitakyushu, Fukuoka, Japan

⁵Institute of Innovative Research, Tokyo Institute of Technology, Yokohama, Kanagawa, Japan

*np.diamantopoulos.pb@hco.ntt.co.jp

Abstract: Record DML-based 325-Gb/s (BTB) and 321.24-Gb/s (2-km SSMF) transmissions are demonstrated based on a >100-GHz bandwidth membrane DML-on-SiC, by utilizing a digitally-preprocessed analog multiplexer and adaptive entropy-loaded DMT modulation, surpassing our previous record by ~34%. © 2020 The Authors

1. Introduction

The surging traffic in data centers pose future standardizations such as Terabit Ethernet (TbE), to rely on line rates in excess of 200-Gb/s [1]. Meanwhile, the per-bit requirements for cost, power consumption, and transceiver footprint are expected to remain strict. These conditions place intensity-modulated and direct-detected (IMDD) systems, and in particular, energy-efficient and wide-bandwidth directly-modulated lasers (DMLs) among the leading technologies to support ICT growth [2-6]. In addition, techniques to expand the electrical modulation bandwidth are urgently required in order to support the fast-growing bandwidth of optical transmitters [7-9].

Recently we presented the first-ever DML capable of >100-GHz bandwidth, based on our novel high-thermal conductivity, membrane-III-V-on-SiC technology and a photon-photon resonance (PPR)-supporting cavity design, which enabled us to achieve record ~240-Gb/s net rates with pulse-amplitude modulation [3]. However, frequency-dependent signal-to-noise ratio (SNR), such as the one caused by PPR [3,4], suggests multi-carrier modulations such as the discrete multi-tone (DMT) [6-7], as an attractive solution. In addition, entropy-loading (EL) [9-11], which relies on probabilistically-shaped (PS) constellations [12] on a sub-carrier/band basis, adds additional flexibility.

In this work, based on a similar III-V/SiC, >100-GHz bandwidth DML [3] and by combining an adaptive EL-DMT modulation with a wide-bandwidth, digitally pre-processed analog multiplexer (AMUX) [7,8], we demonstrate net 325-Gb/s and 321.24-Gb/s at back-to-back (BTB) and after 2-km of standard single-mode fiber (SSMF) transmissions, respectively, surpassing our previous net rate by ~34%. To the best of our knowledge, these results set new records for energy-efficient and low-cost DML-based optical interconnections based on a single laser.

2. Membrane III-V-on-SiC DML

The DML was based on our membrane-III-V-on-SiC technology and had a similar cavity design to the one in [3]. The III-V layer was based on InGaAlAs multi-quantum wells that were directly-bonded through a SiO₂ layer to the SiC substrate prior to the laser fabrication. The total III-V thickness was ~340 nm. Such a membrane structure enables high optical confinement, while the high thermal conductivity of the SiC substrate ensures a high differential gain at high current densities; both of which contribute to high relaxation oscillation frequencies [3]. Single-mode operation

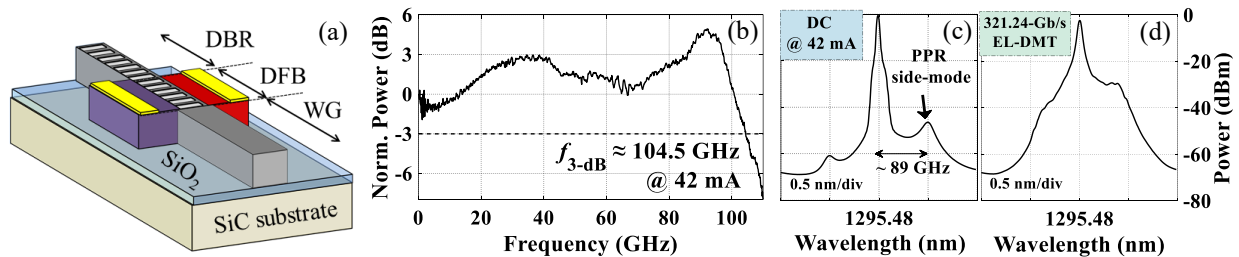


Fig. 1: >100-GHz DML: (a) schematic, (b) E/O response, spectra for (c) 42-mA DC and (d) 321.24-Gb/s EL-DMT DFB: distributed feedback; DBR: distributed Bragg grating; WG: waveguide; PPR: photon-photon resonance.

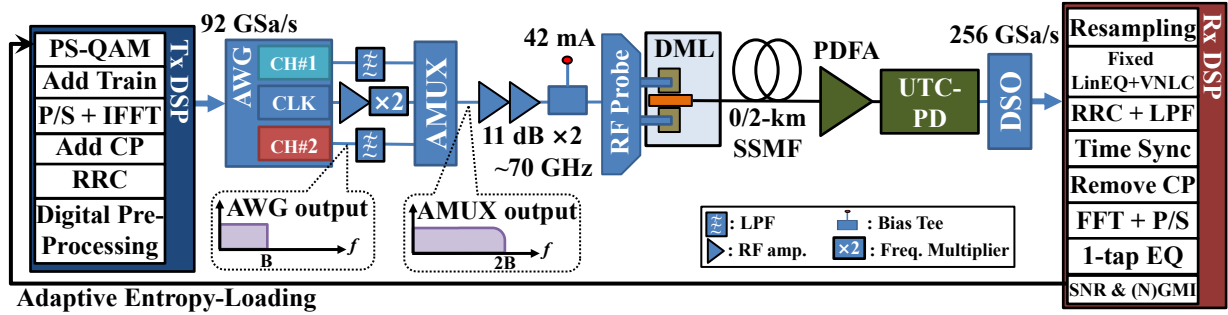


Fig. 2: Experimental setup; AMUX: Analog Multiplexer; CLK: Clock; LPF: Low-Pass Filter; RRC: Root-Raised Cosine; CP: Cyclic Prefix; (I)FFT: (inverse) Fast-Fourier Transform; EQ: Equalizer; VNLC: Volterra filter.

was provided by the distributed reflector design (Fig. 1(a)), consisting of an (active) 50- μm distributed feedback (DFB) and a (passive) 60- μm distributed Bragg reflector (DBR) section, while a 135- μm waveguide (WG) was used for the passive-feedback mechanism generating the PPR. At a bias current of 42 mA and a stage-controlled room temperature of 25 $^{\circ}\text{C}$, the laser exhibited a 3-dB bandwidth of ~ 104.5 GHz (Fig. 1(b)) and a fiber-coupled power of ~ 0.6 dBm at a lasing wavelength of ~ 1295.48 nm (Fig. 1(c)). The side mode suppression ratio was >40 dB, while the PPR side-mode was spaced at ~ 89 GHz. At these conditions the operating power was (42 mA \times 4.233 V \approx) 0.178 W.

3. Experimental demonstration

The experimental setup including the offline digital signal processing (DSP) flowchart is shown in Fig. 2. To drive the AMUX, two ~ 40 -GHz digitally-preprocessed baseband signals and a 41-GHz clock were generated by an arbitrary waveform generator (AWG) at ~ 92 GSa/s. The detailed operation principle of the AMUX and its digital pre-processing are described in [7]. To provide sufficient driving voltage (V_{pp}) to the DML, two ~ 70 -GHz, 11-dB-gain RF drivers were used in tandem prior to a ~ 70 -GHz bias-tee connected to an RF probe via a short RF cable. In order to detect the ~ 80 -GHz bandwidth signal, an in-house uni-travelling-carrier photodiode (UTC-PD) was used together with a praseodymium-doped fiber amplifier (PDFA) to provide sufficient 9.1 dBm received optical power (ROP) as in [3]. To monitor the precise ROP and spectrum at the Rx, a 20 dB optical coupler (not shown) was placed prior to the PD. The signals were then stored by a >100 -GHz real-time digital sampling oscilloscope (DSO) at 256-GSa/s. Note that, the use of PDFA can be omitted by increasing the laser's launched power through further optimization of our III-V/SiC technology to take better advantage of the SiC's high thermal conductivity and by integrating the laser with a spot-size converter for low-loss fiber-coupling [13]. In addition, integration of the PD with a trans-impedance amplifier or use of PDs with better receiver sensitivity can reduce the required ROP effectively.

The DMT had a sampling rate of $R_s = 160$ GSa/s, $N_{sub} = 512$ subcarriers, and a total cyclic-prefix (CP) and training overhead of $\sim 1.9\%$ (combined rate, $r_{CP+Train} = 0.9814$). The main DMT processes were similar to the ones in [6]. A 0.01-rolloff root-raised cosine (RRC) filter was used for pulse shaping at the transmitter (Tx) with a similar matched filter at the receiver (Rx). At the Rx DSP, the signals were first resampled at $2R_s$ and then equalized by a fixed (pre-trained) linear Wiener filter and an 11-tap 3rd-order Volterra nonlinear compensator (VNLC) followed by a low-pass filter (LPF) to remove residual clock components. Regarding the EL profile, at first, fixed (non-PS) 256-, 64-, and 16-quadrature-amplitude modulations (QAM) were attributed to the subcarriers based on their QPSK-probed SNRs (Fig. 3(b)-(c)). Subcarriers with SNR < 5 dB were not used. Then, the entropies $H(X_i)$ were optimized iteratively based on a vectorial Newton's method for a given normalized generalized mutual information (NGMI) [14] target. The "effective" NGMI as described for multi-carrier modulations [9] was used as the main performance metric. Whereas previous methods relied on 3D look-up tables [11] –which require computationally-intensive simulations to be generated and have limited entropy resolutions–, our (machine-learning-based) approach has the advantage of rapid-convergence (less than 5 iterations were used) with arbitrary small resolution and small computational burden. Note that, the adaptation doesn't have to be repeated after the initialization of the system and no power loading is necessary.

The effective NGMI versus the net and pre-forward error correction (FEC) data rates are summarized in Fig. 3(a) for BTB and 2-km SSMF transmissions. The net rates are based on a concatenated FEC with an aggregate overhead (OH) of $\sim 21\%$ (total code rate, $r_{FEC} = 0.826$) and an NGMI threshold of 0.857 [15]. Hence the net rate here is given by $NetRate = r_{FEC} * r_{CP+Train} * R_s / 2N_{sub} * \sum_i H(X_i)$. Based on this 0.857 NGMI threshold, net 325-Gb/s and 321.24-Gb/s were achieved after BTB and 2-km SSMF transmissions, respectively. The pre-FEC rates (after removing the CP+Train OH) were 388.91 Gb/s and 393.46 Gb/s, respectively. The SNRs, entropies, (N)GMIs (per-subcarrier), and the electrical spectrum after the Rx-DSP filtering of the 321.24-Gb/s EL-DMT signal after 2-km SSMF are shown

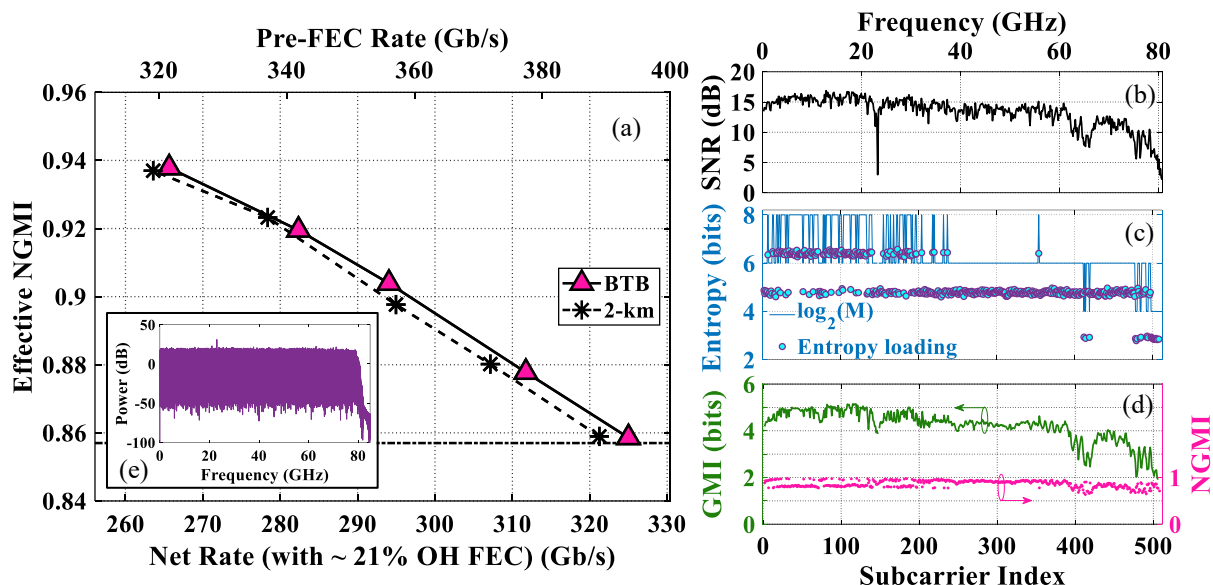


Fig. 3: (a) Effective NGMI vs. Data Rate and (b) QPSK-probed SNR, (c) Entropy-loading, (d) (N)GMI per subcarrier, (e) electrical spectrum after VNLC+RRC+LPF for 321.24-Gb/s EL-DMT after 2-km.

in Fig. 3(b)-(e), respectively. Also the modulated optical spectrum after the DML is shown in Fig. 1(d). In this case, the average SNR was ~ 13.3 dB. The SNR dip around 23-GHz (148-th subcarrier) corresponds to residual clock components seen as spurs in the electrical spectrum of Fig. 3(e), and we think it was probably caused by the AWG, (i.e., $92/4 = 23$ GHz).

Future works will be focused on optimizing our III-V/SiC technology to increase the laser's fiber-coupled fiber and also co-integrate the laser with the high-speed electronics.

4. Conclusions

Towards low-cost and energy-efficient TbE and short-reach optical interconnections, we have demonstrated record DML-based net 325-Gb/s at BTB and 321.24-Gb/s after 2-km SSMF transmission. The DML transmitter was based on a PPR-enhanced >100 -GHz bandwidth membrane DML-on-SiC, while wide-band, adaptive entropy-loaded DMT modulation was utilized through a digitally-preprocessed analog multiplexer. To the best of our knowledge these results set new records for DML-based IMDD transmissions.

5. References

- [1] "2019 Ethernet Roadmap" <https://ethernetalliance.org/technology/2019-roadmap/>, accessed 20-Feb-2020.
- [2] S. Matsuo and T. Kakitsuka, "Low-operating-energy directly modulated lasers for short-distance optical interconnects," *Adv. Opt. Photonics* **10**(3), 567-643 (2018).
- [3] S. Yamaoka, *et al.*, "239.3-Gbit/s Net Rate PAM-4 Transmission Using Directly Modulated Membrane Lasers on High-Thermal-Conductivity SiC," in *Proc. ECOC'19*, paper PD.2.1.
- [4] Di Che, *et al.*, "Direct Modulation of a 54-GHz Distributed Bragg Reflector Laser with 100-GBaud PAM-4 and 80-GBaud PAM-8," in *Proc. OFC'20*, paper Th3C.1.
- [5] C. Kottke, *et al.*, "High Speed 160 Gb/s DMT VCSEL Transmission Using Pre-equalization," in *Proc. OFC'17*, paper W4L.7.
- [6] N. P. Diamantopoulos, *et al.*, "Energy-Efficient 120-Gbps DMT Transmission using a 1.3- μm Membrane Laser on Si," in *Proc. OFC'18*, paper M2D.5.
- [7] H. Yamazaki, *et al.*, "IMDD Transmission at Net Data Rate of 333 Gb/s Using Over-100-GHz-Bandwidth Analog Multiplexer and Mach-Zehnder Modulator," *J. Lightwav. Technol.* **37**(8), 1772-1778 (2019).
- [8] H. Yamazaki, *et al.*, "Net-400-Gbps PS-PAM transmission using integrated AMUX-MZM," *Opt. Express* **18**(27), 25544-25550 (2019).
- [9] Xi Chen, *et al.*, "Single-Wavelength and Single-Photodiode Entropy-Loaded 554-Gb/s Transmission over 22-km SMF," in *Proc. OFC'19*, paper Th4B.5.
- [10] Di Che and W. Shieh, "Approaching the Capacity of Colored-SNR Optical Channels by Multicarrier Entropy Loading," *J. Lightwav. Technol.* **36**(1), 68-78 (2018).
- [11] Di Che and W. Shieh, "Squeezing out the last few bits from band-limited channels with entropy loading," *Opt. Express* **27**(7), 9321-9329 (2019).
- [12] F. Buchali, *et al.*, "Rate Adaptation and Reach Increase by Probabilistically Shaped 64-QAM: An Experimental Demonstration," *J. Lightwav. Technol.* **34**(7), 1599-1609 (2016).
- [13] H. Nishi, *et al.*, "Membrane distributed-reflector laser integrated with SiO_x-based spot-size converter on Si substrate," *Opt. Express* **24**(16), 18346-18352 (2016).
- [14] J. Cho, *et al.*, "Normalized Generalized Mutual Information as a Forward Error Correction Threshold for Probabilistically Shaped QAM," in *Proc. ECOC'17*, paper M.2.D.2.
- [15] T. Kobayashi, *et al.*, "35-Tb/s C-band Transmission over 800 km Employing 1-Tb/s PS-64QAM signals enhanced by Complex 8×2 MIMO Equalizer," in *Proc. OFC'19*, paper Th4B.2.